

Antiferromagnetic quantum criticality in $\text{CeCoGe}_{2.1}\text{Si}_{0.9}$ under pressure

M. Alzamora,^{1,*} M. B. Fontes,² J. Larrea J.,² H. A. Borges,¹ E. M. Baggio-Saitovitch,² and S. N. Medeiros³

¹*Departamento de Física, Pontifícia Universidade Católica do Rio de Janeiro, M. S. de Vicente 225, CEP 22.453-900 Rio de Janeiro, RJ, Brazil*

²*Centro Brasileiro de Pesquisas Físicas, Rua Xavier Sigaud, CEP 22290-180 Rio de Janeiro, RJ, Brazil*

³*Departamento de Física, Universidade Estadual de Maringá, Avenida Colombo 5790, CEP 87020-900 Maringá, PR, Brazil*

(Received 27 February 2007; revised manuscript received 10 May 2007; published 10 September 2007)

We report on the disappearance of antiferromagnetic order in $\text{CeCoGe}_{2.1}\text{Si}_{0.9}$ as seen by electrical resistance measurements. The Néel temperature decreases monotonically with pressure, following Doniach's phase diagram for Kondo lattice systems, and vanishes at the critical pressure $P_C \approx 6.2$ kbar. The electrical resistivity in the vicinity of P_C shows clearly a non-Fermi-liquid behavior. Beyond that, the system recovers its truly Fermi-liquid state. The nature of this canonical phase diagram is given in a semiquantitative discussion based on two-dimensional spin fluctuations coexisting with a moderate disorder.

DOI: [10.1103/PhysRevB.76.125106](https://doi.org/10.1103/PhysRevB.76.125106)

PACS number(s): 71.27.+a, 71.10.Hf, 62.50.+p, 72.10.Di

I. INTRODUCTION

The study of the ground state of strongly correlated f electron systems, such as the Kondo lattice (KL) systems, is currently of intense interest in the contemporary condensed matter physics. It is mainly focused on the anomalous physical properties close to the borderline between magnetically ordered and nonmagnetic ground states, i.e., close to a magnetic quantum critical point (QCP).¹ This quantum phase transition can be accessed by means of an appropriate tuning control parameter, such as pressure (P), magnetic field (B), or doping (x), that drives the magnetic ordering temperature $T_m \rightarrow 0$ K. The quantum fluctuations in the vicinity of this magnetic instability play an important role in the formation of states such as the non-Fermi-liquid (NFL) and the unconventional superconductivity.^{1,2}

Usually, the physics of the magnetic ground state of KLs can be described by Doniach's phase diagram,³ which accounts for the competition between Ruderman-Kittel-Kasuya-Yosida (RKKY) and Kondo interactions, both depending on the same coupling constant J between the local moments and the itinerant electrons. In the nonmagnetic side, this phase diagram is supplemented by a coherence line which marks the onset of Fermi-liquid (FL) behavior.⁴ This extended description establishes the universality of a class of canonical phase diagrams, whose experimental realization can be observed in many P -tuning phase diagrams of clean Ce-based KL systems, much more frequently in antiferromagnetic^{1,5} (AF) than ferromagnetic (FM) quantum critical points.^{6,7} Despite the fact that the physical properties in the vicinity of a QCP are described by physical laws which depend on the type of magnetic instability, the physical scenario in the QCP does not depend on the type of magnetic order and, thus, is expected to be universal.^{1,8-10}

It is crucial for the understanding of the QCPs to elucidate the clear existence of the magnetic moments.⁸⁻¹⁴ If the magnetic moments persist at the QCP, the competition between Kondo screening and long-range interactions leads to local as well as long wavelength degrees of freedom, and both can be critical near the QCP.¹² On the other hand, if they are quenched by Kondo screening at a finite Kondo temperature

(T_K) when the critical control parameter (J_C) is reached, then the criticality is governed by the long wavelength fluctuations of the magnetic moments at the QCP. Kondo compensation plays also an important role in the case of strong disorder, where rare configurations of magnetic moments lead to the formation of magnetic clusters dominated by quantum fluctuations near the QCP.¹⁴ The latter degree of freedom may not only modify the physical laws of the NFL regime but also induce some peculiarities in the canonical phase diagram close to the QCP, as seen in the case of x -tuning magnetic instability.^{15,16}

$\text{CeCoGe}_{2.1}\text{Si}_{0.9}$ is an antiferromagnetic KL system with a moderate $\gamma = 133$ mJ/mol K² and Néel temperature (T_N) ≈ 4 K.¹⁷ This compound crystalizes in the tetragonal BaNiSn_3 type structure and belongs to the family of $\text{CeCoGe}_{3-x}\text{Si}_x$, where the suppression of antiferromagnetism occurs at $x_C = 1.2$.¹⁷ Considering the proximity of the $\text{CeCoGe}_{2.1}\text{Si}_{0.9}$ system close to the x_C and the equivalence for the volume compression ($\Delta V/V$) dependence between P - and x -tuning experiments, one should expect that the $\text{CeCoGe}_{2.1}\text{Si}_{0.9}$ system can be driven to a magnetic instability, and beyond that, to a paramagnetic regime under moderate values of pressure.¹⁷ So, the study of P -phase diagram of this system becomes very interesting not only for the properties of the P -tuned QCP, but also for the relevant information that this study provides for understanding the x -tuned phase diagram of the CeCoGe_3 type compounds very close to its x -tuned QCP.

This paper reports electrical resistivity, $\rho(T)$, measurements under hydrostatic pressures ($P < 11$ Kbar) on the polycrystalline $\text{CeCoGe}_{2.1}\text{Si}_{0.9}$ antiferromagnetic-KL compound. Our aim is to study the P -tuning phase diagram and to find out the physical mechanisms associated with the QCP, if they really exist. Since our present $\rho(T)$ measurements have been performed down to very low temperatures and at higher pressures than those previously reported for the $\text{CeCoGe}_{2.25}\text{Si}_{0.75}$ compound,¹⁸ our findings may provide a better characterization of the type of magnetic QCP and also an understanding of the AF quantum criticality proposed for the $\text{CeCoGe}_{3-x}\text{Si}_x$ system.

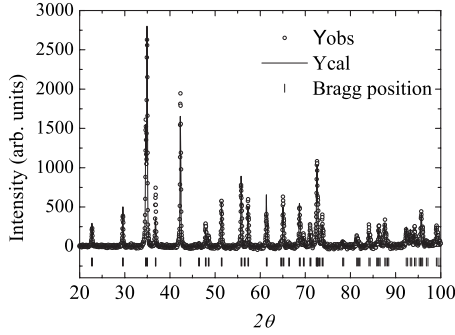


FIG. 1. The x-ray diffraction pattern of $\text{CeCoGe}_{2.1}\text{Si}_{0.9}$ polycrystalline. The solid line is the fit obtained from Rietveld analysis.

II. EXPERIMENTAL DETAILS

The $\text{CeCoGe}_{2.1}\text{Si}_{0.9}$ polycrystalline material was prepared by arc melting stoichiometric amounts of pure elements from Alfa Aesar (Ce, 4N; Co, 4N; Ge, 5N; and Si, 5N+) under argon atmosphere and then heat treating the sample at 900 °C for seven days in argon-filled quartz tubes. The x-ray diffraction (see Fig. 1) shows the correct lattice structure, and the Rietveld analysis provided the cell parameters $a=b=4.270(2)$ Å and $c=9.765(3)$ Å, free from foreign phases within the resolution limit of 5% of the technique. The electrical resistance $R(T)$ experiments were performed in a piston-cylinder pressure (PCP) cell for $P < 12$ kbar, with fluorinert FC75 as pressure transmitting medium and the conventional four-probe ac method. The electrical contacts were made with Pt wire 25 μm in diameter and silver epoxy. A lead strip is employed as a pressure manometer. The $R(T)$ measurements were carried out for two different batches of samples with the same PCP setup and yielding similar results. This pressure cell is inserted in a $\text{He}^3\text{-He}^4$ dilution refrigerator that allows to reduce the temperature down to 50 mK. We used a calibrated Cernox temperature sensor, from Lake Shore, located in the bottom, but inserted in a cavity of the pressure cell. The experiment were made during heating, with rate of 10–15 mK/min and stability better than 0.2 mK. Moreover, the regular geometry of the bulk sample, $290 \times 510 \times 800$ μm³, allows one to estimate accurately the electrical resistivity.

III. RESULTS AND DISCUSSION

A. Electrical resistance measurements

Normalized electrical resistivity data $\rho(T)/\rho(300\text{ K})$ for $\text{CeCoGe}_{2.1}\text{Si}_{0.9}$ at some selected pressures are shown in Fig. 2. At ambient pressure, the residual resistivity ratio (RRR) $\rho_{300\text{ K}}/\rho(T \rightarrow 0\text{ K}) \sim 4$ falls into an expected magnitude as that reported in Ref. 17 for the concentration regimen between $x=0.5$ and 1.0. However, the residual resistivity in our compound $\rho_0 \sim 74$ μΩ cm is 25% larger. Although the RRR is a typical value for the present $\text{CeCoGe}_{2.1}\text{Si}_{0.9}$ material, the value of the residual resistivity is larger than that of most clean Ce-based Kondo lattices. This suggests the presence of atomic disorder which may influence the electronic and magnetic correlations near a magnetic instability.

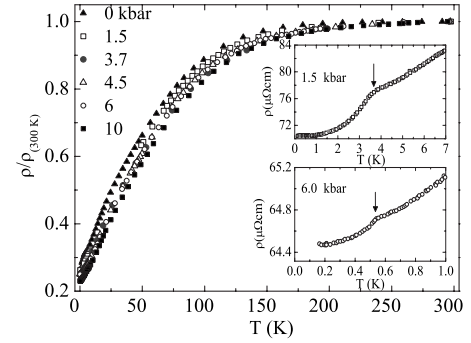


FIG. 2. The normalized electrical resistivity $\rho(T)$ data $\rho/\rho(300\text{ K})$ of $\text{CeCoGe}_{2.1}\text{Si}_{0.9}$ at different pressures. Inset: two representative resistivity curves at lower temperatures. The arrows indicate the onset of the AF ordering state.

Figure 2 shows some features of the basic interactions of the ground state. The overall shape of $\rho(T)$ shows a slow decrease with temperature which is enhanced around 150 K. This behavior suggests a large crystal-field splitting (Δ'), i.e., $T_K < \Delta'$, so one should expect that the influence of the crystalline electric field (CEF) on the physical properties at low temperatures can be safely neglected. The inset of Fig. 2 shows the magnetic ordering temperature (T_N), indicated by arrows, which is associated with a clear-cut bend at low temperatures. The precise position of T_N is determined from the minimum in the second derivative of the smoothed resistivity data shown in Fig. 3, and it is plotted as a function of pressure in Fig. 4. As obtained from previous magnetic and specific heat measurements,¹⁷ T_N marks the onset of antiferromagnetic order. Further evidence for the presence of an AF ordering state can be inferred from the spin-wave-based analysis of the $\rho(T)$ data for $T < T_N$, as discussed below.

Signs of magnetic order can only be observed up to 6 kbar. Beyond that, the electrical resistivity at low T shows either a nearly linear or a quadratic T dependence at different ranges of temperature, scaling as $\rho(T) \propto T^n$, where $1 < n \leq 2$. As shown in Fig. 5 for $P=6.7$ kbar, two different effective exponents are revealed from a fit in a logarithmic scale of $\Delta\rho(T) = \rho - \rho_0 \propto T^n$: $n=2$, from the lowest measuring tempera-

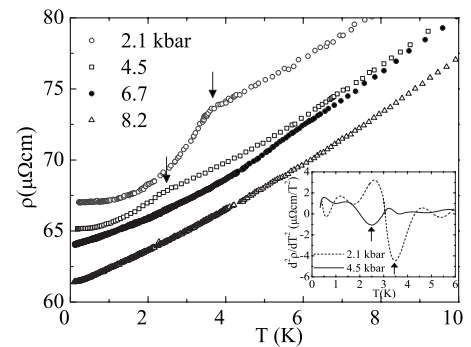


FIG. 3. Some resistivity curves at lower temperatures for different pressures. The arrows indicate the onset of the AF ordering state. Inset: evaluation of T_N from the minimum of the second derivative of the resistivity data for $P=2.1$ and 4.5 kbar.

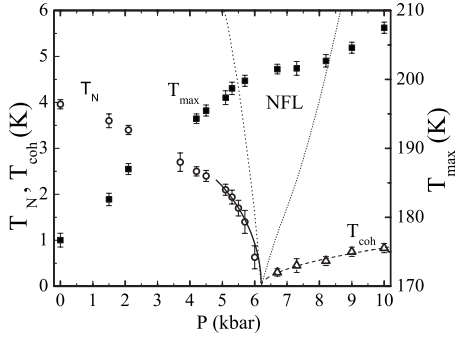


FIG. 4. Phase diagram of $\text{CeCoGe}_{2.1}\text{Si}_{0.9}$ as function of pressure taken from our $\rho(T)$ measurements, with $P_C \approx 6.2(2)$ kbar. The critical (full) and coherence (dashed) lines are power laws with mean-field exponents, and T_{max} is the temperature of the maximum in ρ_m (see text). The shaded region represents the NFL regime according to our $\rho(T)$ analysis.

tures up to the coherence temperature T_{coh} , as in a nonmagnetic FL; and $n=1.10(5)$, from above T_{coh} extending over more than one decade of temperatures, suggesting a NFL state. The combination of those findings gives clear evidence of the existence of a quantum critical point at the critical pressure P_C , close to 6 kbar. Since our experiments have been performed in small pressure steps around 6 kbar, showing a smooth decrease of T_N , we can estimate P_C with good precision using the mean-field approximation $T_N \propto |\delta|^{1/2}$, where $|\delta| = |P - P_C|$. This fit, over a large pressure range, yields a critical line $T_N(P)$ and $P_C = 6.2(2)$ kbar defining the QCP.

Another interesting aspect related to the quantum critical behavior in our compound can be inferred by means of the pressure evolution of the Kondo state. In order to do that, it is convenient to separate the magnetic contribution to the resistivity, ρ_m , by subtracting the phonon contribution ρ_{ph} from the measured data. In our case, ρ_{ph} can be roughly estimated using the empirical relation $\rho_{ph}(T) \approx [0.1(1) \mu\Omega \text{ cm/K}]T$,¹⁹ which is expected to be negligible at temperatures below 4 K ($\rho_{ph} \approx 0.4 \mu\Omega \text{ cm}$) by comparison with $\rho(T)$ large residual resistivity.

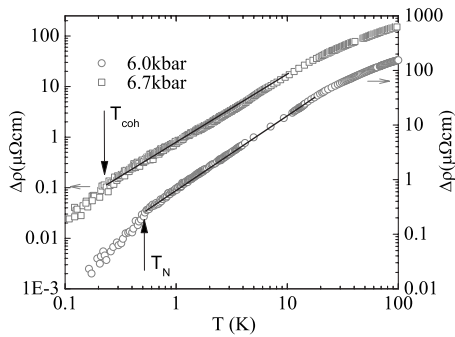


FIG. 5. Logarithmic plot of $\Delta\rho(T)$, where the solid lines show T^n dependence over more than one decade in T associated with a NFL behavior, where $n=1.27(5)$ (at $P=6$ kbar) and $n=1.10(5)$ (at $P=6.7$ kbar). The coherence (T_{coh}) and Néel (T_N) temperatures are indicated by arrows.

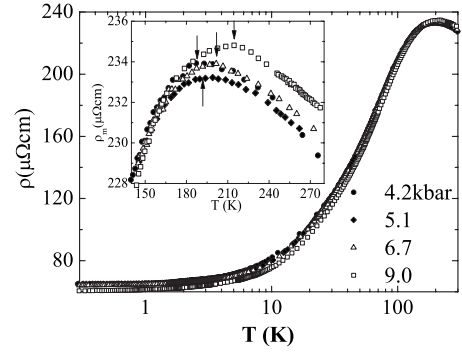


FIG. 6. Magnetic resistivity ρ_m vs T in a logarithmic scale for $\text{CeCoGe}_{2.1}\text{Si}_{0.9}$ at different pressures. The arrows indicate the temperature where ρ_m is maximum, T_{max} .

Figure 6 shows the overall shape of $\rho_m(T)$ as a function of $\ln T$ at different pressures. The most important feature observed is the broad peak with a $\ln T$ -like tail above 150 K, which is a typical behavior of a Kondo lattice influenced by a CEF interaction.²⁰ T_{max} , defined by the center of the peak, moves to higher values as pressure increases. In the scope of the Kondo lattice model,²⁰ $T_{max} \propto T_K$ and is plotted as a function of P in Fig. 4. In the framework of Doniach's phase diagram,³ the profile of $T_{max}(P)$ is associated with the increase of the Kondo screening contribution due to the enhancement of the hybridization between the Ce $4f$ and the itinerant electronic states. According to recent full potential local orbital basis band structure calculations²¹ performed for CeCoGe_3 type of compounds, these itinerant electrons could mainly arise from the $3d$ Co electronic band. Such a case is compatible with our findings, shown in Fig. 4, since the increase of the Kondo screening results in the decrease of the long-range magnetic ordering (LRMO) state.

It is also noteworthy that the value of P_C found in our experiments leads to a volume compression $\Delta V/V = 0.62\%$, which is 50% smaller than that expected in $\text{CeCoGe}_{3-x}\text{Si}_x$ system considering the x -tuning experiments from $x=0.9$ to $x_C=1.2$, and a constant compressibility $\kappa = (\Delta V/V)/(\Delta P) = 1 \times 10^{-3} \text{ kbar}^{-1}$. The κ value can be inferred from Ref. 17, with the assumption that the volume compression of 10% is equivalent to the application of an external pressure as high as 100 kbar if only the Ce sublattice is taken into account. It turns out that under pressure, T_N drops to zero at a much smaller volume compression than under Si substitution. This supports the assumption of effective electronic changes in the $\text{CeCoGe}_{3-x}\text{Si}_x$ series, leading to a crossover to intermediate valence, which can only be reached at pressures much higher than our present experimental conditions.¹⁷ This fact suggests that in $\text{CeCoGe}_{2.1}\text{Si}_{0.9}$, the suppression of the AF order by pressure is related to an antiferromagnetic QCP rather than an intermediate valence transition, as we will discuss below.

B. Antiferromagnetic phase

Figure 4 shows a partial dome shape of the $T_N(P)$, i.e., T_N decreases continuously with pressure, which can be qualita-

tively explained in the framework of the Doniach model³ for KL systems. In this model, the phase diagram results from the competition between the Kondo effect $T_K \propto \exp(-1/|J|)$ and the RKKY interaction $T_N \propto J^2$. So, the shape of $T_N(P)$ arises mainly from two correlated aspects: the large value of J in the ground state of $\text{CeCoGe}_{2.1}\text{Si}_{0.9}$, because this system is close to a magnetic instability in the $\text{CeCoGe}_{3-x}\text{Si}_x$ series,¹⁷ and the subsequent P increase of J due to enhancement of the hybridization between the local Ce $4f$ magnetic moments and the itinerant electron states. On the other hand, the obtained values of T_N in our experiments show a smooth decrease instead of a sharp drop close to P_C . This profile close to P_C looks very similar to other AF Kondo lattices near an antiferromagnetic QCP.^{1,5,22} This fact might discard a discontinuous behavior of $T_N(P)$ typical of a first order transition.²³ In the following, we give further evidence of AF ordering state in our system using a spin-wave (SW) approach, which complements the lack of magnetic measurements close to P_C .

A clear indication of magnetic ordering are the kinks in the $\rho(T)$ curves for $P \leq 6$ kbar (inset of Figs. 2 and 3), which can be identified as T_N . The continuous decrease of T_N with P indicates that $\text{CeCoGe}_{2.1}\text{Si}_{0.9}$ is driven toward a plausible AF-QCP. So, other aspects about quantum criticality can be inferred from the magnetic phase, below 6 kbar and below $T_N(P)$. The low energy magnetic excitations (magnons or spin waves) scatter the conduction electrons, giving rise to a magnetic contribution $\rho_m(T)$ to the resistivity which in our system is nearly equal to $\rho(T)$ for $T < 4$ K. Therefore, the magnetic resistivity data at low temperatures are given by $\rho_m(T) = \rho_0 + \rho_{\text{SW}}(T) + mT^n$. ρ_{SW} is the spin-wave contribution and the second term mT^n , with $1 < n \leq 2$, accounts for the electron-electron (ee) scattering.^{6,24–27} In anisotropic antiferromagnets, the dispersion relation of the hydrodynamic spin-wave modes is given by $\omega(k) = \sqrt{\Delta^2 + Dk^2}$, where Δ is the SW gap and D the SW stiffness. The magnon gap is due to the magnetic anisotropy arising from the peculiarities of the magnetic structure of the CeCoGe_3 type compounds and the high anisotropy of the electronic f states.^{7,17,23,28,29} For $k_B T < \Delta$, one finds for $\rho_{\text{SW}}(T)$:¹⁸

$$\rho_{\text{SW}} = C \left(\frac{\Delta}{k_B} \right)^{3/2} T^{1/2} e^{-\Delta/k_B T} \left[1 + \frac{2}{3} \left(\frac{k_B T}{\Delta} \right) + \frac{2}{15} \left(\frac{k_B T}{\Delta} \right)^2 \right], \quad (1)$$

where the coefficient C is related to the spin-wave stiffness by $D \propto 1/C^{2/3}$ or $\Gamma \propto 1/C^{1/3}$, where Γ is the effective magnetic coupling between Ce ions.

The resistivity data were fitted for $T_{\text{fit}} \leq 0.6T_N$ [Fig. 7(a)], where ρ_0 is taken as the only fixed parameter. One can see, for pressures $P \leq 5.7$ kbar, that the spin-wave contribution to $\rho_m(T)$ dominates, being still relevant at pressures nearly below P_C . In the particular case of $P=0$ (not shown here), the value of $m=0.27 \mu\Omega \text{ cm K}^{-2}$ obtained from a FL contribution ($n=2$) leads to a ratio $m/\gamma^2 = 1.2 \times 10^{-5} \mu\Omega \text{ cm} [\text{mol K}(\text{mJ})^{-1}]^2$. This value is typical of heavy fermions (HFs) with degeneracy of quasiparticles (QPs) $N=2$, i.e., most of the degeneracy is lost because of

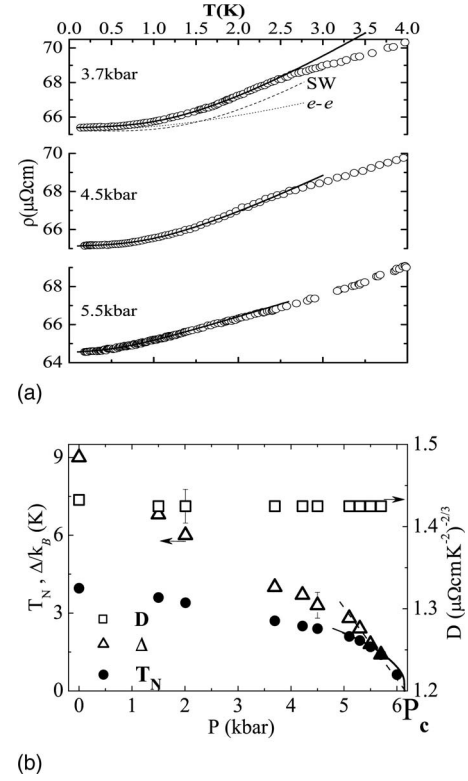


FIG. 7. (a) $\rho_m(T)$ of $\text{CeCoGe}_{2.1}\text{Si}_{0.9}$ at very low T . Solid lines are the fits using Eq. (1). At $P=3.7$ kbar, we show the SW and ee (with $n=2$) contributions, respectively (see text). (b) Pressure dependence of Δ , D , and T_N parameters for $P \leq 6.2$ kbar. The solid line is obtained from Eq. (2) considering a gap Δ (dashed line) and $\Gamma/k_B \sim 2.6$ K (see text).

the large crystal-field splitting Δ' .³¹ These aspects guarantee that the values obtained from the fits for the gap Δ and the parameter C are quite reliable. Figure 7(b) shows the pressure dependence of the gap $\Delta(P)$, the stiffness $D(P)$, and $T_N(P)$. There is a clear correlation between $T_N(P)$ and $\Delta(P)$. Both decrease with pressure, suggesting the collapse of the LRMO as $\text{CeCoGe}_{2.1}\text{Si}_{0.9}$ approaches the QCP. In particular, the gap decreases linearly with pressure and with the same rate as T_N close to P_C . An extrapolation of $\Delta/k_B \rightarrow 0$ K yields the same critical pressure as before, $P_C \approx 6.2$ kbar.

It is noteworthy in Fig. 7(b) that the bare spin-wave stiffness $D(P)$ remains nearly unchanged in the whole investigated P range and is probably finite down to P_C . Under this consideration, the disappearance of T_N as the QCP is approached cannot be explained only by a softening of the spin waves. In the spin-wave approach, this can occur if the magnetic excitations are two dimensional (2D) and, in agreement with the experiments, they become isotropic at the QCP. In this case, the vanishing of the spin-wave gap at P_C drives the magnetic instability. This scenario was previously proposed to describe the P -induced AF-QCPs in $\text{CeCoGe}_{2.25}\text{Si}_{0.75}$ (Ref. 18) and YbFe_2Ge_2 ,²³ and the FM-QCP transition for CePt .⁷ Independent of the type of magnetic QCP, it is possible to establish a relationship between $T_{N/C}(P)$ and $\Delta(P)$, where $\Delta(P) \propto |\delta| = |P - P_C|$ is taken as a control parameter. For a $d=2$ system, there is long-range order at finite tempera-

tures only in the presence of a spin-wave gap. In the particular case of an AF system ($S=1/2$), the critical temperature is given by¹⁸

$$k_B T_N = \frac{2\Gamma}{\sqrt{1 + (\Delta/T)^2 \ln\{1 + [\pi^2/2(\Delta/T)^2]\}}} \quad (2)$$

and $T_N \rightarrow 0$ when $\Delta \rightarrow 0$. So, choosing a pressure range where $D(P)$ is nearly constant and since $\Gamma \propto \sqrt{D}$ and $\Delta(P) = 2.57|P-6.2|$ as obtained from the ρ_m data, the only free adjustable parameter in Eq. (2) is Γ . This yields $\Gamma/k_B = 2.6$ K, a value comparable with Γ for other HFs with magnetic-QCP transitions.^{7,23,27} As shown in Fig. 7(b), the critical line $T_N(P)$ is reproduced in a considerable range of pressures far from the QCP. Since our results for $T_N(P)$ can be described by Eq. (2), the present mechanism of the unquenched magnetic moments down to the QCP, together with a soft gap and 2D magnetic excitations, gives an alternative physical scenario for the quantum criticality of CeCoGe_{2.1}Si_{0.9} on the magnetic regime.

A qualitative understanding of these results can be obtained within the f - d hybridization model of Endstra *et al.*³⁰ for similar heavy-fermion systems, with a characteristic hybridization matrix $|V_{df}|$. The anisotropy is strongly connected to the f character of the wave function of the local electrons. As V_{df} increases, there is a strong admixture of these states into the d states, which have quenched orbital moments. Consequently, as V_{df} increases, the wave functions of the electrons responsible for the magnetism become much less anisotropic, decreasing the spin-wave gap. This qualitative scenario for the P -induced QCP in CeCoGe_{2.1}Si_{0.9} could also be extended to the CeCoGe_{3-x}Si_x type compounds close to the vanishing of the AF ordering state at the critical concentration $x_C=1.2$. In this case, the substitution of the Si by Ge atoms not only could increase f - d hybridization but also it might increase the Ge/Co site disorder. Together, both may induce a strong modification mainly in the f - d hybridizations,²¹ thus, reducing progressively the magnetic anisotropy when the system approaches the magnetic instability.

The assumption that the local magnetic moments of Ce remain unquenched down to the QCP is consistent with neutron scattering in the Ce systems CeRh₂Si₂ (Ref. 26) or CeCu_{6-x}Au_x (Ref. 12) that show the presence of local magnetic moments of Ce ions even at the QCP. At present, there is still a lack of knowledge about the magnetic structure of CeCoGe_{2.1}Si_{0.9}, either in single or in polycrystals. A suitable comparison with the isostructural CeCoGe₃ system provides strong arguments in favor of the two-dimensional character of the magnetic excitations in our system. The collinear AF ordering along the c axis in CeCoGe₃ promotes the interactions between Ce ion neighbors in basal planes perpendicular to the c direction. The reduction of the dimensionality of the low-lying excitations from three dimensions to two dimensions is a paradigm in the physics of the QCP.¹ One dramatic consequence of this is the possible formation of states, such as unconventional superconductivity, in the vicinity of the QCP. However, our present $\rho(T)$ experiments do not show

any sign of superconductivity around P_C , at least down to 50 mK.

C. Quantum critical point and its concomitant non-Fermi-liquid behavior

As seen in Fig. 5, a careful analysis of $\rho(T)$ around $P_C = 6.2$ kbar shows a dependence like $T^{1.27(5)}$ ($P=6$ kbar) and $T^{1.10(5)}$ ($P=6.7$ kbar), from nearly above T_N or T_{coh} , respectively, and extending over two decades in temperature. That indicates the development of a NFL behavior in both sides of the phase diagram very close to P_C , giving a strong evidence of the existence of a QCP. Considering the temperature and pressure ranges where NFL behavior sets in, the limits of the NFL regime can be plotted as seen in Fig. 4. In general, in the spin fluctuation framework for an AF instability, the resistivity has a temperature dependence $\rho(T) \propto T^\beta$, with $\beta = d/z$, $1 < \beta < 2$, and $d+z > 4$. Here, d is the dimensionality of the spin fluctuations and z the dynamic exponent.^{11,32} So, for a system near an antiferromagnetic instability at P_C , with $z=2$, one expects to find $\beta=3/2$ for three dimensions and $\beta=1$ for two dimensions.³² Comparing with other β values found for HF systems close to an AF-QCP,^{23,25} and considering the error bar of the exponents determined by the fit in Fig. 5, the NFL behavior found in CeCoGe_{2.1}Si_{0.9} suggests that this system is governed by two-dimensional antiferromagnetic spin fluctuations. However, for the present case, the small deviation from the predicted value $\beta=1$ in the NFL behavior does not discard the importance of atomic disorder. Such a NFL behavior arises in the Griffiths phase scenario, where rare configurations due to magnetic disorder dominates the physics. These are large nearly ordered clusters which, however, do not percolate. These large clusters have a quantum critical character and give rise to NFL behavior.¹⁴ The formation of a Griffiths phase due to a strong disorder has been invoked to explain the unusual muon spin relaxation (μ SR) results found in the x experiments on CeCoGe_{3-x}Si_x system close to AF instability.³³ Strong disorder at the critical concentration $x_C=1.2$ yields to the formation of AF clusters embedded in a paramagnetic environment which accounts for the concomitant NFL behavior. Notice that for CeCoGe_{2.1}Si_{0.9}, the value of the residual resistivity $\rho_0(P=0) \sim 74 \mu\Omega$ cm is quite large in comparison to clean HFs,¹ supporting the role of disorder in this system. The influence of disorder is generally seen as a deviation from the linear T dependence of the resistivity in the NFL regime, as a pressure regime with NFL behavior, or as an irreversibility in the electrical resistivity when the system crosses back through the QCP.¹⁴⁻¹⁶ In our case, only the first is observed, suggesting that if local atomic disorder exists, it is moderate and might coexist with other mechanisms in the vicinity of P_C .

Further aspects of the quantum criticality in CeCoGe_{2.1}Si_{0.9} system can be obtained from the analysis of $\rho(T)$ in the nonmagnetic (NM) regime, i.e., above $P_C > 6.2$ kbar. The electrical resistivity scales as $\Delta\rho(T) = AT^2$, as is appropriate to a FL state, from the lowest temperatures up to a limiting temperature T_{coh} . As seen in Fig. 4, the increase of T_{coh} with pressure is a clear indication that our system

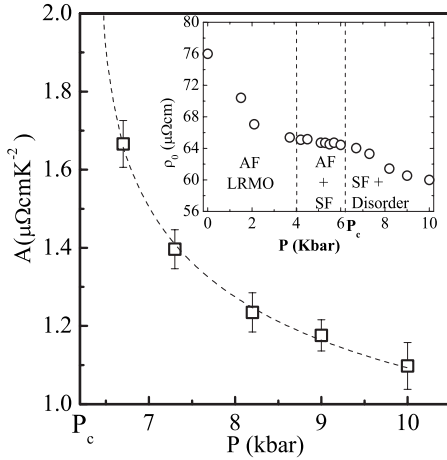


FIG. 8. Pressure dependence of the coefficient A of the T^2 term of the resistivity above the QCP ($P_C=6.2$ kbar) for $\text{CeCoGe}_{2.1}\text{Si}_{0.9}$. Inset: Residual resistivity ρ_0 as a function of P . The dotted lines separate different regimes named according to the $\rho_0(P)$ behavior: antiferromagnetic ordering (AF), AF quantum critical regime (AF+SF), and coexistence of disorder and SF (D+SF) in the nonmagnetic side.

moves away from the QCP. A similar aspect can be inferred from Fig. 8, which shows the T^2 coefficient as a function of pressure. $A(P)$ exhibits a moderate decrease from pressures close to, but above, the QCP, up to 8 kbar, after which it decreases slower. The behavior of both $T_{coh}(P)$ and $A(P)$ indicates that the system is being tuned away from the quantum critical region and is in agreement with the theoretical predictions for the nonmagnetic side of the phase diagram of heavy fermions.^{4,11} However, in comparison to other HF systems close to a magnetic QCP,^{6,23,24} the rate of decrease of $A(P)$ nearly above the QCP (see Fig. 8) suggests that the expected divergence of $A(P)$ with $|P-P_C|^{-n}$ is quite weak. This is confirmed by the fit $A(P) \propto 1/|\delta|^{0.21(1)}$ in the vicinity of the QCP, as shown in Fig. 8. Even considering the error bar for this exponent, the obtained value $n \sim 0.2$ is considerably different from the lowest value $n=1/2$ predicted by the spin fluctuations (SFs) theory for a system either in the local or nonlocal critical regime of a magnetic QCP.^{7,11,23} In the present case, the reduction of the exponent n may be associated with the presence of disorder, which might alter the QP-QP scattering cross section, suggesting that the whole Fermi surface undergoes no singular scattering at P_C .^{24,29} On the other hand, the experimental values of T_{coh} fall in a range of temperatures quite low and have no linear P dependence near the QCP. A similar profile of $T_{coh}(P)$ observed in Fig. 4 was found in the nonmagnetic regime of $\text{CeCoGe}_{3-x}\text{Si}_x$ phase diagram,³⁴ but with huge values of T_{coh} . However, since the volume compression induced by P for $\text{CeCoGe}_{2.1}\text{Si}_{0.9}$ is substantially smaller than those by x -tuning experiments on $\text{CeCoGe}_{3-x}\text{Si}_x$, we can expect that the small values of $T_{coh}(P)$ seen in Fig. 4 correspond to those values of $T_{coh}(x)$ in the local quantum critical regime, i.e., very close to the x -tuning QCP. In addition, the nonlinear P dependence of T_{coh} seen in Fig. 4 suggests that $T_{coh}(P)$ can be well described by a mean-field term, i.e., by $T_{coh} \propto |\delta|^{1/2}$.

D. Residual resistivity

The inset of Fig. 8 shows the pressure dependence of the residual resistivity $\rho_0(P)$, which was estimated from the average value of the resistivity between $T \sim 0.05$ and 0.15 K for all pressures. The resulting error bars are rather small in comparison to the absolute ρ_0 values. As seen in the inset of Fig. 8, $\rho_0(P)$ decreases monotonically with P for $P < 4$ kbar, remaining nearly constant up to $P_C=6.2$ kbar. Beyond that pressure, it starts to decrease again. This profile of $\rho_0(P)$ in the vicinity of the QCP looks different than those of other HF systems close to a magnetic instability governed by valence as well as spin fluctuations.^{6,23,35} As is usually expected for many Ce-based KL systems, the transition from magnetic to nonmagnetic regime is accompanied by a valence transition from localized Ce^{3+} to an intermediate valence $\text{Ce}^{3+ \leftrightarrow 4+}$, resulting in an increase of the residual resistivity due to the enhancement of valence fluctuations. However, the $\rho_0(P)$ profile seen in the inset of Fig. 8 shows that the $\text{CeCoGe}_{2.1}\text{Si}_{0.9}$ system is located far from the valence intermediate regime, at least up to the presently investigated pressure range $P < 11$ kbar. An attempt to explain this unusual $\rho_0(P)$ can be done as follows.

At lower pressures ($P < 4$ kbar), the continuous P decrease of ρ_0 is consistent with the reduction of the scattering process by the Ce local magnetic moments due to the enhancement of the Kondo screening. In the range of pressures nearly below the QCP, the change of $\rho_0(P)$ toward a nearly constant P dependence arises from the strong increase of the electronic relaxation time and is, in turn, related to the critical spin fluctuations.²³ In the NM regime, the subsequent decrease of $\rho_0(P)$ could only be explained by assuming a reduction of the critical spin fluctuations, which are partially quenched by the coexistence of uncorrelated local moments (short-range-ordered spin clusters) and a paramagnetic region, i.e., the formation of Griffiths phase.^{14,33} Such a scenario for $\text{CeCoGe}_{2.1}\text{Si}_{0.9}$ is compatible with the disordered $\text{CeCoGe}_{3-x}\text{Si}_x$ series, where the random substitution of Si atoms at $2a$ and $4b$ sites of Ge and disorder at nominal Ge/Co sites are the reasons of atomic disorder. Thus, the very important atomic disorder in $\text{CeCoGe}_{2.1}\text{Si}_{0.9}$, which can be considered as static disorder, acquires a dynamical character when the system approaches the QCP, making possible the coexistence of this mechanism with the spin fluctuation in the quantum critical regime.

IV. CONCLUSIONS

The analysis of the $\rho(T)$ data shows that the application of pressure on the $\text{CeCoGe}_{2.1}\text{Si}_{0.9}$ KL system induces an antiferromagnetic QCP at $P_C \approx 6.2(2)$ kbar. At the magnetic side, our $\rho_m(T)$ data can be well described by AF spin waves. We can adopt a model where two-dimensional magnons become isotropic or gapless at P_C , giving rise to a magnetic instability at the same pressure. This model successfully accounts for our experimental results and even allows us to obtain a numerical value for the bare exchange interaction between the unquenched local moments along the relevant planes in the ordered magnetic phase. In the nonmagnetic regime, the

T dependence of the resistivity ascribed to a NFL behavior together with unexpected P dependence of A and ρ_0 , nearly above P_C , is a clear evidence that the 2D AF spin fluctuation would not be the only driving force to account for the AF quantum criticality in our system. In addition to that, the coexistence with noncorrelated magnetic clusters as a Griffiths phase becomes necessary to be taken into account. However, our findings suggest that the dynamical disorder induced by P may be considered as moderate. It would be very useful to perform neutron scattering and μ SR experiments in our system in order to confirm the behavior with

pressure of the spin-wave parameters and the influence of disordered in the nonmagnetic regime. Also, Hall effect experiments in single crystals could help to elucidate the change of the nature of the quasiparticles due to the disorder.

ACKNOWLEDGMENTS

We thank M. A. Continentino for helpful discussions. This work is partially supported by PRONEX/FAPERJ, FAPERJ/Cientista do Nosso Estado, CAPES CT-Energy, PADCT-FAPERJ, and CNPq.

*mariella@cbpf.br

- ¹For a review see G. Stewart, *Rev. Mod. Phys.* **73**, 797 (2001).
- ²C. Pfeleiderer, D. Reznik, L. Pintschovius, H. V. Löhneysen, M. Garst, and A. Roch, *Nature (London)* **427**, 227 (2004).
- ³S. Doniach, in *Valence Instability and Related Narrow Band Phenomena*, edited by R. D. Parks (Plenum, New York, 1977), p. 169.
- ⁴M. A. Continentino, G. M. Japiassu, and A. Troper, *Phys. Rev. B* **39**, 9734 (1989).
- ⁵G. Knebel, D. Braithwaite, P. C. Canfield, G. Lapertot, and J. Flouquet, *Phys. Rev. B* **65**, 024425 (2001).
- ⁶J. Larrea J., M. B. Fontes, A. D. Alvarenga, E. M. Baggio-Saitovitch, T. Burghardt, A. Eichler, and M. A. Continentino, *Phys. Rev. B* **72**, 035129 (2005); J. Larrea J., T. Burghardt, A. Eichler, M. Fontes, A. D. Alvarenga, and E. Baggio-Saitovitch, *J. Magn. Magn. Mater.* **272**, 52 (2004).
- ⁷S. Drotziger, C. Pfeleiderer, M. Uhlarz, H. v. Löhneysen, D. Souptel, W. Löser, and G. Behr, *Phys. Rev. B* **73**, 214413 (2006).
- ⁸J. Hertz, *Phys. Rev. B* **14**, 1165 (1974).
- ⁹A. J. Millis, *Phys. Rev. B* **48**, 7183 (1993).
- ¹⁰T. Moriya and T. Takimoto, *J. Phys. Soc. Jpn.* **64**, 960 (1995).
- ¹¹For a review see T. Moriya, *Spin Fluctuations in Itinerant Electron Magnetism* (Springer, Berlin, 1985).
- ¹²A. Schröder, G. Aeppli, R. Coldea, M. Adams, O. Stockert, H. V. Löhneysen, E. Bucher, R. Ramazashvili, and P. Coleman, *Nature (London)* **407**, 351 (2000); Q. Si, S. Rabello, K. Ingersent, and J. L. Smith, *ibid.* **413**, 804 (2001); P. Coleman and A. J. Schofield, *ibid.* **433**, 226 (2005).
- ¹³F. M. Grosche, P. Agarwal, S. R. Julian, N. J. Wilson, R. K. W. Haselwimmer, S. J. S. Lister, N. D. Mathur, F. V. Carter, S. S. Saxena, and G. G. Lonzarich, *J. Phys.: Condens. Matter* **12**, L533 (2000).
- ¹⁴A. H. Castro Neto, G. Castilla, and B. A. Jones, *Phys. Rev. Lett.* **81**, 3531 (1998); A. Rosch, *ibid.* **82**, 4280 (1999); E. Miranda, V. Dobrosavljevic, and G. Kotliar, *J. Phys.: Condens. Matter* **8**, 9871 (1996).
- ¹⁵J. G. Sereni, T. Westerkamp, R. Küchler, N. Caroca-Canales, P. Gegenwart, and C. Geibel, *Phys. Rev. B* **75**, 024432 (2007).
- ¹⁶R. Chau and M. B. Maple, *J. Phys.: Condens. Matter* **8**, 9939 (1996).
- ¹⁷Duhwa Eom, Masayasu Ishikawa, Jiro Kitagawa, and Naoya Takeda, *J. Phys. Soc. Jpn.* **67**, 2495 (1998).
- ¹⁸M. A. Continentino, S. N. de Medeiros, M. T. D. Orlando, M. B. Fontes, and E. M. Baggio-Saitovitch, *Phys. Rev. B* **64**, 012404 (2001).
- ¹⁹H. Wilhelm and D. Jaccard, *Phys. Rev. B* **66**, 064428 (2002).
- ²⁰B. Cornut and B. Coqblin, *Phys. Rev. B* **5**, 4541 (1972); D. L. Cox and N. Grewe, *Z. Phys. B: Condens. Matter* **71**, 321 (1988).
- ²¹T. Jeong, *Solid State Commun.* **141**, 316 (2007).
- ²²See D. Belitz, T. R. Kirkpatrick, and Thomas Vojta, *Rev. Mod. Phys.* **77**, 579 (2005).
- ²³J. Larrea J., M. B. Fontes, E. M. Baggio-Saitovitch, J. Plessel, M. M. Abd-Elmeguid, J. Ferstl, C. Geibel, A. Pereira, A. Jornada, and M. A. Continentino, *Phys. Rev. B* **74**, 140406(R) (2006).
- ²⁴P. Gegenwart, J. Custers, C. Geibel, K. Neumaier, T. Tayama, K. Tenya, O. Trovarelli, and F. Steglich, *Phys. Rev. Lett.* **89**, 056402 (2002).
- ²⁵N. D. Mathur, F. M. Grosche, S. R. Julian, I. R. Walker, D. M. Freye, R. K. W. Haselwimmer, and G. G. Lonzarich, *Nature (London)* **394**, 39 (1998).
- ²⁶T. T. M. Palstra, A. A. Menovsky, and J. A. Mydosh, *Phys. Rev. B* **33**, 6527 (1986).
- ²⁷A. Demuer, D. Jaccard, I. Sheikin, S. Raymond, B. Salce, J. Thomasson, D. Braithwaite, and J. Flouquet, *J. Phys.: Condens. Matter* **13**, 9335 (2001).
- ²⁸V. K. Pecharsky, O.-B. Hyun, and K. A. Gschneidner, Jr., *Phys. Rev. B* **47**, 11839 (1993).
- ²⁹A. Thamizhavel, T. Takeuchi, T. D. Matsuda, Y. Haga, K. Sugiyama, R. Settai, and J. Onuki, *J. Phys. Soc. Jpn.* **74**, 1858 (2005).
- ³⁰T. Endstra, G. J. Nieuwenhuys, and J. A. Mydosh, *Phys. Rev. B* **48**, 9595 (1993); V. K. Pecharsky, O. B. Hyun, and K. A. Gschneidner, *ibid.* **47**, 11839 (1993).
- ³¹N. Tsujii, H. Kontani, and K. Yoshimura, *Phys. Rev. Lett.* **94**, 057201 (2005).
- ³²C. Pfeleiderer, G. J. McMullan, S. R. Julian, and G. G. Lonzarich, *Phys. Rev. B* **55**, 8330 (1997).
- ³³V. V. Krishnamurthy, K. Nagamine, I. Watanabe, K. Nishiyama, S. Ohira, M. Ishikawa, D. H. Eom, T. Ishikawa, and T. M. Briere, *Phys. Rev. Lett.* **88**, 046402 (2002).
- ³⁴K. Kanai, T. Terashima, D. H. Eom, M. Ishikawa, and S. Shin, *Phys. Rev. B* **60**, R9900 (1999).
- ³⁵D. Jaccard, H. Wilhelm, K. Alami-Yadri, and E. Vargoz, *Physica B* **259-261**, 1 (1999); J. Larrea J., M. B. Fontes, E. M. Baggio-Saitovitch, M. M. Abd-Elmeguid, C. Geibel, and M. A. Continentino, *J. Phys. Soc. Jpn.* (to be published).